École Polytechnique Fédérale de Lausanne
Laboratoire de Physique des Hautes Énergies - Spring semester 2019

TP IVb Project:

Feasibility Studies for a Measurement of the Charm Mixing Parameter y_{CP} Using Full LHCb Data

Author: *Anna Mascellani*

Supervisor: *Guillaume Pietrzyk*

Contents

1 Introduction

The weak interactions of the Standard Model (SM) induce an asymmetry between the behaviour of some particles and their CP counterparts, known as CP violation (CPV). Effects of CPV were first observed in the 1960s at Brookhaven Laboratory in the US in neutral K mesons. In 2001, experiments at the SLAC laboratory in the US and the KEK laboratory in Japan also observed the phenomenon in neutral B mesons. The first evidence of CPV in D^0 mesons was obtained in March 2019 by the LHCb collaboration at CERN [1].
CP violation is an essential feature of the universe, responsible for the abundance of matter over antimatter that we observe today. Since the level of CPV in the Standard Model's weak interactions is too small to account for the present-day matter-antimatter imbalance, a source of CPV beyond the SM needs to be identified. With much improved precision, the effect of such a new source might be found in heavy-flavour meson decays.
This analysis is inserted in the context of CPV measurements in the charm sector. In particular, all the studies here presented are related to the measurement of the y_{CP} mixing parameter in neutral charmed meson decays. Most part of the analysis is then dedicated to the study of the detector efficiency and its incidence on these measurements.
Since the value of y_{CP} is extracted from event distributions as functions of the decay-time, one of the main issues in terms of detection efficiency is here related to low-lifetime mesons. Indeed, in an experiment like LHCb at CERN, a D^0 meson with zero lifetime will decay exactly at the collision point, where the rate of events is too high to obtain a reliable measurement of the decay of interest. In addition, if the meson travels for a too short distance, its decay products easily mix with background events and are thus excluded from the signal. In light of this, quantifying the effects of the detector efficiency on the performed measurements is a key point in the results interpretation.
This report is divided into three main sections. The first will present the theoretical background, introducing the concepts of CPV and y_{CP} in the charm sector. Then, section 3 will describe the procedure used to measure y_{CP} from simulated samples of D^0 meson decays with an efficiency correction applied. Lastly, two different studies on the detector efficiency will be performed and reported.

2 Theory and Motivation

This first section aims to provide a theoretical background for the studies that will be performed and explained in the following. After a brief discussion about discrete symmetries and CP violation in the SM, the effects of CPV will be further investigated with regard to their manifestation in the mixing rates of neutral mesons. Subsequently, the discussion will concentrate on the charm sector and on the definition of y_{CP} for D^0 meson decays.

2.1 Discrete Symmetries and CP Violation in the Standard Model

The description of the existing types of particles and their different interactions is based on continuous symmetries of the Standard Model Lagrangian. However, other discrete transformations that generate further symmetries also exist and are key to the understanding of fundamental characteristics of the universe, such as the prevalence of matter over anti-matter. Three such transformations are parity (P), reversing the spatial coordinates $\bar{x} \to -\bar{x}$ and thus switching the particle chirality; charge conjugation (C), which transforms each particle in its anti-particle by changing the sign of all quantum numbers; and time reversal (T), which reverses the temporal coordinate $t \to -t$. One of the basic principles of physics, expressed in the CPT theorem, states that every Lorentz invariant theory must also be invariant under the combination CPT of these three transformation, although it does not have to be invariant under the individual application of each of them.
Since matter and anti-matter were created in equal quantities in the early universe, the above-mentioned current disparity between them implies the violation of the invariance under the exchange of a particle with its anti-particle. In 1973, when only the first two generations of quarks were known, two Japanese physicists, Makoto Kobayashi and Toshihide Maskawa, proposed that a new generation of quarks was needed to incorporate CPV within the SM. They introduced a unitary matrix, now called the Cabibbo-Kobayashi-Maskawa (CKM) matrix, which describes the strength of flavour-changing weak decays with 4 free parameters. 3 of them consist of mixing angles, while the fourth one is a CP-violating complex phase [2]. However, the level of CPV permitted in the SM through the CKM mechanism is too small to account for all of the current disparity between particles and antiparticles. Thus, further studies of CPV may reveal Beyond the SM physics to account for it.

2.2 CP Violation in Mixing of Neutral Mesons

The neutral mesons K^0, D^0, B_d^0 and B_s^0 consist of a quark and an antiquark, both up-type (up, charm, tau) or down-type (down, strange, beauty) but with different flavours. As they are neutral, they can change flavour and turn into the corresponding anti-mesons via charged weak interactions, as shown for example in Figure 1 for the D^0 meson. This phenomenon, known as flavour oscillation or mixing in the neutral mesons, occurs because the eigenstates of the Hamiltonian governing the time evolution of the system do not correspond to the flavour eigenstates which result from the interaction. Thus, we can write the Hamiltonian

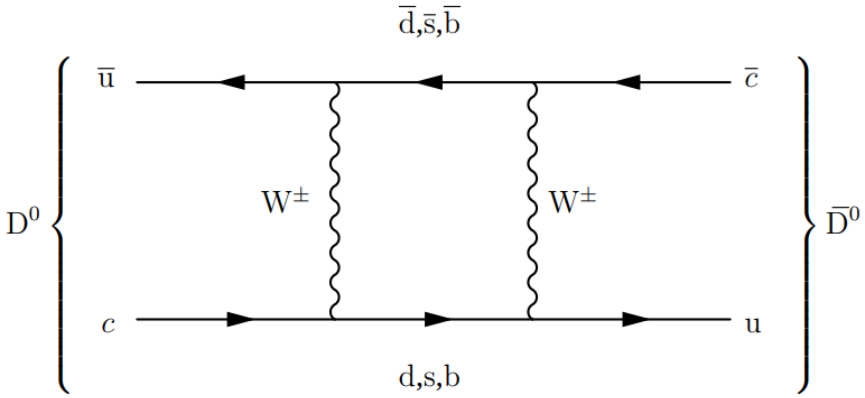

Figure 1: One of the dominant diagrams contributing to D^0 mixing.

eigenstates $|D_{1,2}\rangle$ as a superposition of $|D^0\rangle$ and $|\overline{D}^0\rangle$

$$|D_{1,2}\rangle = p\,|D^0\rangle \pm q\,|\overline{D}^0\rangle \tag{1}$$

where p and q are two complex parameters satisfying the normalization condition $|p|^2+|q|^2 = 1$.
In the limit of CP conservation, p is equal to q and the Hamiltonian eigenstates correspond to the CP eigenstates. Furthermore, in this case, the neutral meson oscillations are characterised by only two dimensionless parameters, $x \equiv (m_1 - m_2)/\Gamma$ and $y \equiv (\Gamma_1 - \Gamma_2)/2\Gamma$, where $m_{1(2)}$ and $\Gamma_{1(2)}$ are the mass and decay width of the CP-even (odd) eigenstate $D_{1(2)}$, respectively, and $\Gamma \equiv (\Gamma_1 + \Gamma_2)/2$ is the average decay width for the D-system. In the presence of CPV, the ratio $|p/q|$ is in general different from 1 and this leads to different mixing rates for states initially produced in different flavour eigenstates - namely D^0 and $\overline{D}^0$. This phenomenon is known as "indirect CP violation" and it further enriches the phenomenology of neutral meson decays [3].

2.3 The Charm Sector and y_{CP}

The level of CPV for the neutral charm mesons predicted by the SM is very small, ($O(10^{-3})$ or less). Significantly greater CPV effects could be achieved through non-Standard-Model processes contributing in the mixing and decay amplitudes. Therefore, high precision measurements in the charm sector may open an outlook to new physics. In addition, study of CPV in the up-type mesons are complementary to those already performed with beauty and strange mesons, thus providing an opportunity to progress in the understanding of the mechanism responsible for the matter anti-matter asymmetry in the universe.
Because of $D^0 - \overline{D}^0$ mixing, the effective decay width Γ_{CP+} of decays to CP-even final states differs from the average decay width Γ, which instead corresponds to final states of undefined CP. Γ_{CP+} is measured in decays of the type $K \to h^+ h^-$ ($h = K, \pi$), while Γ in decays that

involve an equal mixture of CP-even and CP-odd states, such as $D^0 \to K^- \pi^+$. To quantify the discrepancy between these two observables, we define the mixing parameter

$$y_{CP} \equiv \frac{\Gamma_{CP+}}{\Gamma} - 1 = \frac{\Gamma(D^0 \to h^+h^-) + \Gamma(\overline{D}^0 \to h^+h^-)}{2\Gamma} - 1 \tag{2}$$

We can relate y_{CP} to the parameter x and y defined in section 2.2 through the quantities $|q/p|$ and $\phi \equiv \arg(q\bar{A}/pA)$ as follows

$$y_{CP} \approx \frac{1}{2}\left[\left(\left|\frac{q}{p}\right| + \left|\frac{p}{q}\right|\right) y\cos\phi - \left(\left|\frac{q}{p}\right| - \left|\frac{p}{q}\right|\right) x\sin\phi\right] \tag{3}$$

where $A\,(\bar{A})$ is the $D^0\,(\overline{D}^0)$ decay amplitude for the $h^+\,h^-$ final state [4]. In the absence of CPV, $|q/p| = 1$ and $\phi = 0$, thus y_{CP} is equivalent to y. Therefore, since any deviation of y_{CP} from y would indicate CPV, improving the precision of both y_{CP} and y measurements might lead to evidences of indirect CPV in $D^0 - \overline{D}^0$ mixing.

3 Simulation of y_{CP} measurements

In this section, a procedure to measure y_{CP} using $D^0 \to K^+K^-$ and $D^0 \to K^-\pi^+$ is described [1]. If one chooses the CP-even final state as $K^+\,K^-$ and the CP-undefined final state as $K^-\pi^+$ in definition 2, then y_{CP} can be redefined as [5]

$$y_{CP} \;=\; \frac{\Gamma(D^0 \to K^+\,K^-)}{\Gamma(D^0 \to K^-\,\pi^+)} - 1 \tag{4}$$

Since only the two final states written above will be considered in the following, we can drop the charges in the products and conveniently write $D^0 \to K\,K$ and $D^0 \to K\,\pi$. With this notation, one can then define the following ratio between the distributions of events for the two decays

$$R \;=\; \frac{N(D^0 \to K\,K)}{N(D^0 \to K\,\pi)} \tag{5}$$

Assuming in both cases and exponential distribution regulated by the decay width of the corresponding channel, $\Gamma(D^0 \to K\,K)$ in one case and $\Gamma(D^0 \to K\,\pi)$ in the other, one can find an expression of R in which y_{CP} appears as an exponential coefficient. Indeed, we can write

$$R \;\propto\; \frac{e^{-\Gamma(D^0\to KK)\,t}}{e^{-\Gamma(D^0\to K\pi)\,t}} \;=\; e^{-(\Gamma(D^0\to KK)-\Gamma(D^0\to K\pi))\,t} \tag{6}$$

which, recalling the definition of y_{CP} in Equation 4, leads to

$$R \;=\; R_0\, e^{-y_{CP}(t/\tau)} \tag{7}$$

where τ corresponds to the effective lifetime of $D^0 \to K\pi$ decays and is given by $\frac{1}{\Gamma(D^0\to K\pi)}$. For each study performed in this analysis, y_{CP} is extracted from an appropriate fit of the distribution for the ratio R, where the latter is obtained from plots of generated samples for $D^0 \to KK$ and $D^0 \to K\pi$ as a function of the D^0 decay time. In the following, a procedure for the measurement of y_{CP} from simulated events of D^0 decays will be described taking into account the presence of a certain efficiency of the detector. Furthermore, a study on the choice of the best fit function for the R plot will be presented.

3.1 Study of the R Observable with an Efficiency Applied

The samples for numerator ($D^0 \to KK$) and denominator ($D^0 \to K\pi$) in the ratio R are generated by picking random numbers from an exponential distribution with a certain effective lifetime ($\tau = 1/\Gamma$). Given the expression of R as a function of y_{CP} in Equation 7, it is convenient to express the decay-time t as a fraction of the $D^0 \to K\pi$ effective lifetime τ; namely, all the plots will be function of t/τ, so that y_{CP} can be directly associated to the

[1] From this point onward, the inclusion of the charge-conjugate decay mode is implied unless otherwise stated.

parameter resulting from the fit of R. The exact value of y_{CP} used to calculate the ratio between the effective lifetimes for the generation is

$$y_{CP} \;=\; 0.00835 \tag{8}$$

which corresponds to the world average value for y_{CP} updated to May 2018 [6]. Since this analysis is based on simulated samples, in the following, this value will be addressed as the expectation value for y_{CP} measurements.
After the generation, a continuous efficiency profile is applied to $D^0 \to K\,K$ and $D^0 \to K\,\pi$ samples. In this first stage, the same efficiency function, corresponding to $\epsilon(t/\tau) = \tanh(t/\tau)$, will be used for both decays. One can notice that by multiplying both numerator and denominator by the same efficiency function, the two contributions cancel out in the ratio

$$\frac{\epsilon(\frac{t}{\tau})N(D^0 \to KK)}{\epsilon(\frac{t}{\tau})N(D^0 \to K\pi)} \;=\; \frac{N(D^0 \to KK)}{N(D^0 \to K\pi)} \;=\; R \tag{9}$$

Thus, even after the efficiency application, one expects to obtain a value of y_{CP} from the fit of the R plot that is compatible with the injected value (8).
If we consider the expression in Equation 7 for R and we expand it in power series, for a small value of y_{CP} we have

$$R \approx 1 - y_{CP}\frac{t}{\tau} \tag{10}$$

For every study performed in this first part of the analysis, the value of y_{CP} is extracted from both an exponential and a linear fit to the R plot. Since the analysis of statistical fluctuations is easier when we deal with linear distributions, here the purpose is to establish whether the linear fit is equivalent to the exponential one for y_{CP} measurements (a more detailed discussion on this will follow in section 3.2).
Figure 2a shows the R plot obtained with samples of $5 \cdot 10^7$ events by filling a histogram with 200 bins for both numerator and denominator decays. It is observed that the errors vary a lot for different bins and are higher for bins with fewer events, namely the ones corresponding to the tails of the exponential distributions. Indeed, assuming a Poissonian distribution for the number of events N in each bin, the corresponding error is computed as $\sqrt{N}$. The uncertainty on the ratio is thus given by

$$\sigma_{\frac{N_1}{N_2}} = \frac{N_1}{N_2}\sqrt{\left(\frac{\sigma_{N_1}}{N_1}\right)^2 + \left(\frac{\sigma_{N_2}}{N_2}\right)^2} \tag{11}$$

where N_1 and N_2 are the number of events in the numerator and denominator bin respectively. Therefore, the lower N_1 and N_2, the higher the error for the bin in the ratio, because the relative uncertainties $\sigma_{N_i}/N_i = 1/\sqrt{N_i}$ $(i = 1, 2)$ decrease with N_i. Therefore, in order to improve the quality of the fit, a rebinning of the histograms is performed so that the errors for different bins become comparable. More specifically, the size of each bin is calculated so that the number of events is approximately the same in each bin of the numerator distribution $(D^0 \to KK)$. The same binning is then maintained for the denominator distribution and the resulting R plot is fitted as in the previous case. Furthermore, the central value of each bin

(in the t/τ axis) is calculated as the average of t/τ ($\langle t/\tau \rangle$) for the distribution of the events within the bin itself. The latter, indeed, can be approximated to a straight line only in the case of a great number of bins, while, for few dozen of bins and an exponentially decreasing plot, the distribution may be significantly different from a linear function, causing its mean value to widely differ from the exact center of the bin. The $\langle t/\tau \rangle$ values are calculated in the numerator plot and used also for the denominator plot, where it is assumed that the bins have very similar averages. Figure 2b shows the R plot obtained with the same samples of Figure 2a but with a variable binning and a total number of 30 bins.

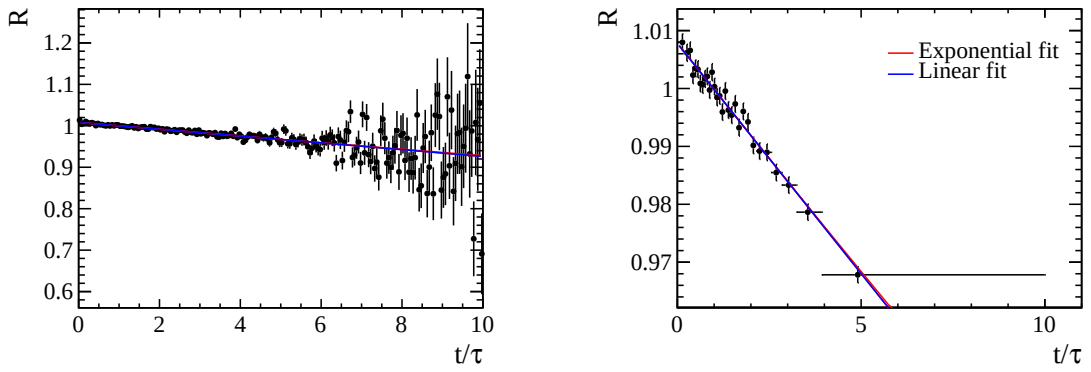

(a) Normal binning. 200 bins.

(b) Variable binning. 30 bins

Figure 2: Plot of the ratio between $D^0 \to KK$ and $D^0 \to K\pi$ distributions as a function of the decay time. The red line corresponds to the exponential fit, while the blue line to the linear one.

3.2 Fit Results for y_{CP}

As already mentioned, the first aim is to verify if it is possible to substitute the exponential fit of the R plot with a linear one. To check this, 1000 studies are performed with different samples to simulate different data collections of the same experiment. Practically, this is accomplished by using each time a different sequence of random numbers to generate the events. For each of these studies, two values of y_{CP} are obtained, one from the exponential fit and the other one from the linear fit. Figure 3 shows the plots for y_{CP} results in the two cases.

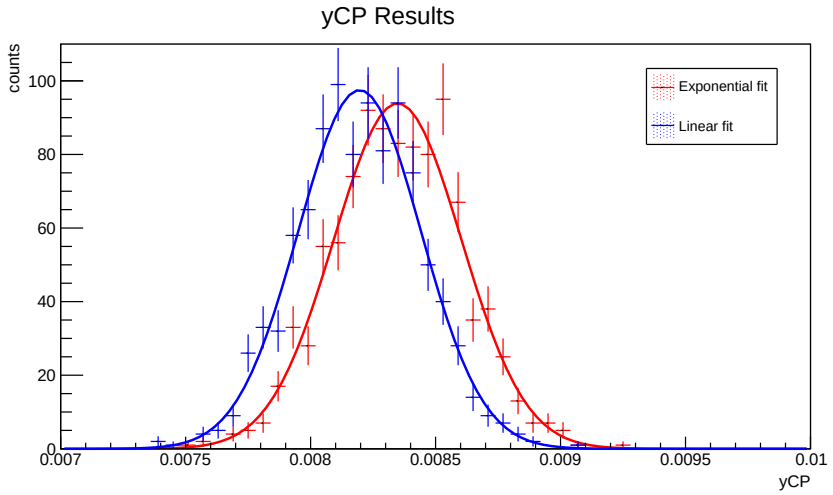

Figure 3: y_{CP} distributions obtained after 1000 studies. The plot in red results from exponential fits, while the blue one results from linear fits of the same R plots.

The final values of y_{CP} are then calculated as the mean over all the parameters resulting from the single fits:

Exponential fit	$y_{CP} = (8.348 \pm 0.008) \cdot 10^{-3}$
Linear fit	$y_{CP} = (8.197 \pm 0.008) \cdot 10^{-3}$

As shown by these results, the distribution obtained with the linear method is shifted leftward with respect to the one produced by exponential fits. Moreover, the mean value from linear fits is incompatible with the expected value of y_{CP} (deviation of 20σ with respect to the value in Equation 8), while, as expected, the exponential method leads to a fully compatible result (deviation of 0.3σ). Thus, we conclude that a linear fit of the R plot does not provide the required precision on the measurement of y_{CP} and in all the following studies the exponential fit function will be adopted.

4 Study of the Detector Efficiency

In this section, two different studies related to the detector efficiency are reported. The first assesses the effect of a certain difference between numerator and denominator efficiency on the measurement of y_{CP}. In particular, a small parameter will be introduced to control this difference and, by progressively varying its value, it will be possible to estimate which is the maximum order of magnitude that we can admit on the difference so that the result on y_{CP} is not compromised. Thus, this kind of analysis allows to quantitatively understand how the variation of the detector efficiency (with respect to different decays) affects the measurement of interest. The second study consists instead in a correction for the efficiency performed on both decays. Two binned efficiency profiles will be used to correct the numerator and denominator samples and certain statistical fluctuations will be introduced on these profiles to verify their incidence on y_{CP} measurements.

4.1 Different efficiencies for different decays

Previously, a method was described to measure y_{CP} from the fit to the R plot when the same efficiency is applied to the two final states considered. Here, the proposed strategy is to progressively vary the efficiency applied to the numerator decay while maintaining unchanged the one used for the generation of the denominator sample and then verify the effect of this variation on the fit results. The functions chosen for the two efficiencies are the following:

$$\begin{aligned} \epsilon_{D^0\to KK}(t/\tau) &= \tanh(t/\tau) + \lambda(1-(2/10)(t/\tau)) \\ \epsilon_{D^0\to K\pi}(t/\tau) &= \tanh(t/\tau) \end{aligned} \tag{12}$$

With this choice, the parameter λ controls the dimension of the variation introduced on the efficiency for $D^0 \to KK$. The study on the measurement of y_{CP} is repeated for different values of λ following the same steps described before. Thus, for each λ, 1000 different samples are created for the two decays and the corresponding values of y_{CP} are returned by exponential fits of R. Table 1 and the graph in figure 4 show the mean value of y_{CP} and its error obtained in correspondence of different values of λ.

λ	y_{CP}
10^{-3}	$(9.215 \pm 0.008) \cdot 10^{-3}$
$5 \cdot 10^{-4}$	$(8.782 \pm 0.008) \cdot 10^{-3}$
10^{-4}	$(8.435 \pm 0.008) \cdot 10^{-3}$
$5 \cdot 10^{-5}$	$(8.391 \pm 0.008) \cdot 10^{-3}$
10^{-5}	$(8.356 \pm 0.008) \cdot 10^{-3}$
$5 \cdot 10^{-6}$	$(8.352 \pm 0.008) \cdot 10^{-3}$
10^{-6}	$(8.348 \pm 0.008) \cdot 10^{-3}$

Table 1

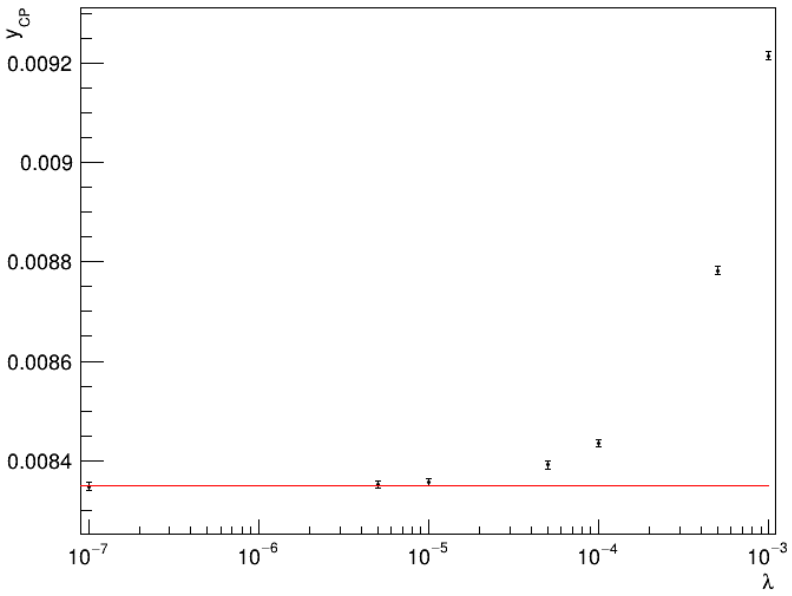

Figure 4: y_{CP} and relative error as a function of λ. The red line in the graph corresponds to the injected value of y_{CP}.

It is found that, by raising λ, the resulting value of y_{CP} increasingly deviates from the expected value (8). In particular, a fully compatible result is obtained for values of λ up to 10^{-5}, while for greater orders of magnitude the agreement is lost: for $\lambda \leq 10^{-5}$ the deviation is lower than 1σ, while for $\lambda \geq 5 \cdot 10^{-5}$ it is higher than 5.1σ.

4.2 Correction for the Efficiency

The procedure described in section 3.1 allows a measurement of y_{CP} from simulated samples of D^0 meson decays with an efficiency applied. To account for this efficiency, the original exponential distributions - which look like the one shown in Figure 5a - were filtered with certain efficiency functions. Thus, the plots of numerator and denominator that were used in the previous studies to calculate the ratio R are similar to the one in Figure 5b (we should here recall that, before calculating the ratio, the two histograms were reshaped with a variable binning, as previously discussed in detail). For the sake of simplicity, in the following, the plots in Figure 5a and 5b will be called *true sample* and *reconstructed sample* respectively.
The purpose of this section is to correct the *reconstructed samples* with certain efficiency profiles by applying weights to the events. By choosing each weight as the inverse of the efficiency for the corresponding decay-time, the exponential behaviour of the *true sample* is indeed recovered for both decays.
This part of the analysis is itself splitted into two different studies. The first one introduces a statistical error on the efficiency used in the correction by fluctuating its value in each bin

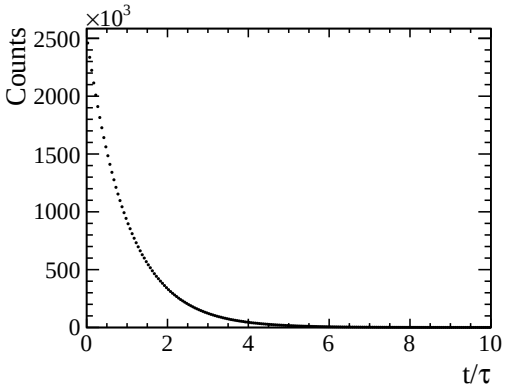

(a) True sample for $D^0 \to KK$.

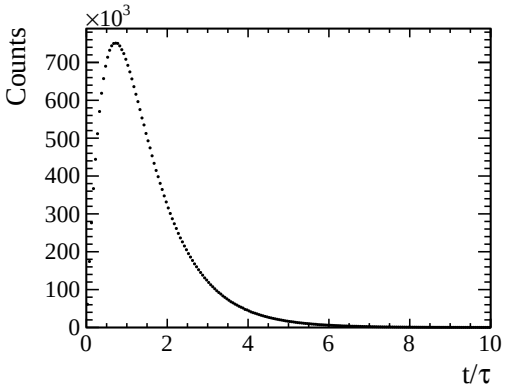

(b) Reconstructed sample for $D^0 \to K\pi$.

Figure 5

within a definite relative uncertainty. In the second study, instead, the efficiency of one of the two decays is varied through correlated fluctuations over the bins and the outcome of this variation is evaluated on the fit results for y_{CP}.

4.2.1 Correction with Statistical Uncertainties on the Efficiency

The correction for the efficiency on the two decays is here performed with the same efficiency functions used in the generation, namely

$$\begin{aligned} \epsilon_{D^0 \to KK}(t/\tau) &= 0.5 \cdot \tanh(t/\tau) + 0.1(1 - (2/10)(t/\tau)) \\ \epsilon_{D^0 \to K\pi}(t/\tau) &= 0.5 \cdot \tanh(t/\tau) \end{aligned} \tag{13}$$

where a difference is maintained between $D^0 \to KK$ and $D^0 \to K\pi$ to account for a possible corresponding variation of the detector efficiency, while the factor 0.5 is conveniently introduced to have $\epsilon(t/\tau) < 1$ in the range $t/\tau \in [0, 10]$. For every y_{CP} study, the following steps are performed:

- Two samples of $5 \cdot 10^7$ events are generated, one for $D^0 \to KK$ and other one for $D^0 \to K\pi$. During the generation, the original exponential distributions are filtered with the two efficiency functions written above (13).
- The correction on the *reconstructed samples* is performed by binning the two efficiency profiles in Eq. 13. More specifically, the efficiency value used in the correction of each bin is randomly extracted from a Gaussian distribution with mean value equal to $\epsilon_i(\langle t/\tau \rangle)$ and standard deviation equal to $\theta \cdot \epsilon_i(\langle t/\tau \rangle)$ (where ϵ_i is the efficiency function in Eq. 13 corresponding to the considered decay, while $\langle t/\tau \rangle$ is the average decay-time within the bin as calculated in the numerator plot). In this way, an uncertainty is introduced for the efficiency and the relative value of this uncertainty is controlled by the parameter

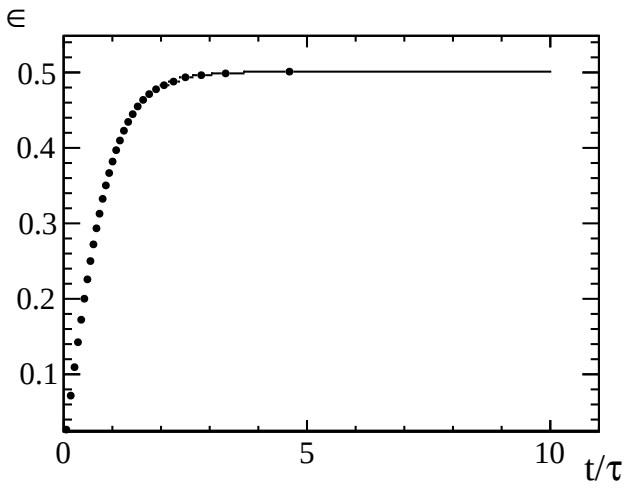

Figure 6: Binned efficiency profile used in the correction of the $D^0 \to K\pi$ plot in one of the y_{CP} studies for $\theta = 10^{-3}$.

θ. An example of binned efficiency profile used in the correction for $D^0 \to K\pi$ is shown in Figure 6.

- Once these values are computed, the same weight is assigned to all the events in the same bin. The weight of a certain bin is calculated as $1/\epsilon_i$. In this way, the original exponential distributions should be recovered.

- Lastly, the R plot obtained from the reconstructed samples is fitted with an exponential function to estimate the value of y_{CP}.

By varying the value of the parameter θ, the uncertainty on the efficiency varies correspondingly. Since the aim of this analysis is to study the incidence of this uncertainty on the measurement of y_{CP}, for each value of θ the same study is repeated several times in order to simulate statistical fluctuations of the efficiency. More precisely, for a certain θ, 1000 y_{CP} studies are performed. For all of them, the same decay samples are maintained, while the efficiency used in the correction of each bin is varied from one study to the other by taking different random numbers from the same Gaussian distribution. Then, as in the previous cases, the final result of y_{CP} is obtained as mean value over all the 1000 fit results.
For $\theta = 0$ (no fluctuation on the efficiency), the fit of the R plot resulting from the considered samples gives the following value of y_{CP}:

$$y_{CP}(0) = (8.646 \pm 0.315) \cdot 10^{-3} \tag{14}$$

With the procedure above described, when θ is non zero, the eventual deviation of the resulting $y_{CP}(\theta)$ with respect to $y_{CP}(0)$ will be solely due to the statistical uncertainties on the efficiency values.

For each θ, the obtained mean value, the standard deviation (σ) and the standard deviation on the mean value (σ_μ) are reported in Table 2 [2]. In addition, the deviation

$$\sigma_{y_{CP}} = y_{CP}(\theta) - y_{CP}(0) \tag{15}$$

is computed as an indication of the bias introduced on y_{CP} measurements by the uncertainty on the efficiency.

θ	$y_{CP}(\theta) \cdot 10^3$	$\sigma_\mu \cdot 10^3$	$\sigma \cdot 10^3$	$\sigma_{y_{CP}} \cdot 10^3$
10^{-2}	8.48	0.08	2.5	-0.16
10^{-3}	8.628	0.008	0.25	-0.018
10^{-4}	8.641	$< 10^{-3}$	0.025	-0.0051
10^{-5}	8.643	$< 10^{-3}$	0.0025	-0.0038
10^{-6}	8.643	$< 10^{-3}$	$< 10^{-3}$	-0.0037

Table 2

4.2.2 Correction with Correlated Fluctuations

In this second part of the analysis, the efficiency functions used as filters while generating the events are the same as before (Equation 13). However, the correction to the *reconstructed samples* are now performed with the introduction of a small variation on one of the two efficiencies. In this way, for the corresponding decay, the efficiency applied as a filter in the generation is slightly different from the one used in the correction. More precisely, two opposite variations are applied to the efficiency for $D^0 \to KK$ through the multiplication of the original profile (as expressed in Equation 13) by the two following linear functions:

$$\begin{aligned} f_1(t/\tau) &= (1+\theta) - (2/10)(t/\tau) \\ f_2(t/\tau) &= 1 + (\theta/10)(t/\tau) \end{aligned} \tag{16}$$

For the $D^0 \to K\pi$ decay, instead, the efficiency used for the correction corresponds to the one applied in the generation. The computation of the efficiency values for single bins is then performed by evaluating the corresponding functions in the average of t/τ within the bin (where the average is always computed in the $D^0 \to KK$ plot).
One can regard the introduced variations as correlated fluctuations of the efficiency values over different bins. The function f_1 introduces a fluctuations whose effect is higher on the first bin and progressively decreases until it vanishes on the last one ($f_1 = 1$ for $t/\tau = 1$). The effect of f_2, on the contrary, is null on the first bin and maximum on the last one. For each θ, two values of y_{CP} are obtained from fits of the R plot: the first (called y_{CP_1} in the results) is related to a study performed with the variation f_1, while the second (y_{CP_2}) is related to the same study but performed with the variation f_2. The decay samples here considered are the same ones used in the analysis described in 4.2.1. Thus, the value of y_{CP} for $\theta = 0$ is the

[2] For 1000 y_{CP} measurements, $\sigma = RMS$, while $\sigma_\mu = RMS/\sqrt{1000}$.

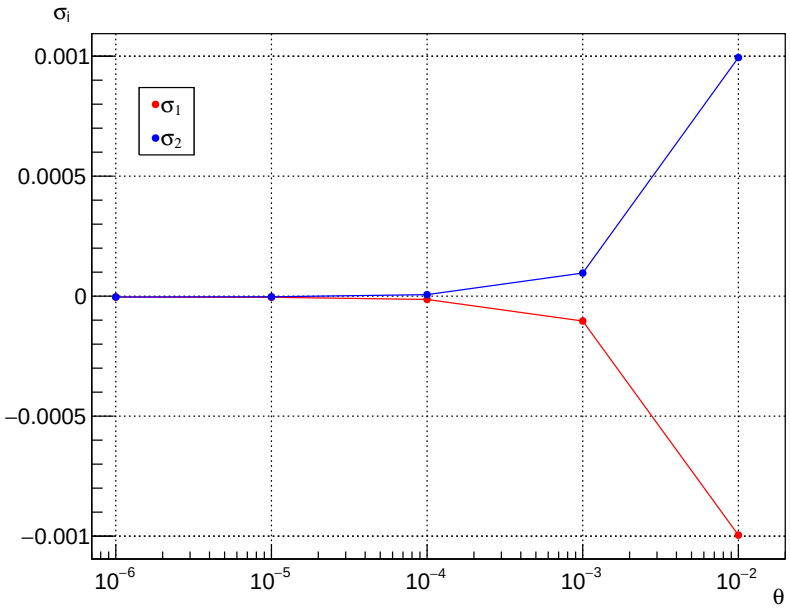

Figure 7: Deviation of $y_{CP}(\theta)$ with respect to $y_{CP}(0)$ introduced by the fluctuations f_1, in red, and f_2, in blue.

same as before (14). To quantify the bias on the measurement of y_{CP} introduced by the two fluctuations at different θ's, the following values are computed:

$$\sigma_i = y_{CP_i}(\theta) - y_{CP}(0) \tag{17}$$

where $i = 1, 2$. The results are reported in Table 3. In addition, the plot in Figure 7 shows the two deviations - σ_1 and σ_2 - as a function of θ.

θ	$y_{CP_1} \cdot 10^3$	$y_{CP_2} \cdot 10^3$	$\sigma_1 \cdot 10^3$	$\sigma_2 \cdot 10^3$
10^{-2}	7.651	9.641	-1.0	0.99
10^{-3}	8.543	8.743	-0.10	0.096
10^{-4}	8.633	8.653	-0.014	0.0063
10^{-5}	8.6417	8.6437	-0.0047	-0.0027
10^{-6}	8.6426	8.6428	-0.0038	-0.0036

Table 3

As previously mentioned, the introduction of f_1 and f_2 controls the impact of efficiency fluctuations at low and high t/τ respectively. The results show that, independently of the value of θ, the bias on y_{CP} (absolute value of σ_i) introduced by f_1 is higher than the one

introduced by f_2. Thus, it is deduced that, in general, a fluctuation at low decay-time is more significant than a similar fluctuation affecting higher regions of the decay-time range. In addition, it is observed that for high value of θ, the two fluctuations cause two opposite deviations: when $\theta \geq O(10^{-4})$, σ_1 is negative, while σ_2 is positive.

5 Conclusions

In this analysis, different studies on the measurement of the charm mixing parameter y_{CP} were performed. For each of them, the value of y_{cp} was extracted from a fit to the ratio between $D^0 \to KK$ and $D^0 \to K\pi$ plots as a function of the D^0 decay-time. To account for the detector efficiency, the samples for the selected final states, initially generated with an exponential distribution, were all filtered with an efficiency function.
In the first stage of the analysis, several y_{CP} measurements were performed using different samples of the two decays and, for each of them, the value of y_{CP} was extracted from both an exponential and e linear fit to the ratio R. The purpose was to verify whether the exponential fit could be replaced by its linear approximation without affecting the measurement of y_{CP}. However, the study showed that the distribution of y_{CP} results obtained with the linear method was shifted leftward with respect to the same distribution produced by exponential fits. In addition, the mean value from linear fits was not in agreement with the expected value of y_{CP} (the one injected during the generation). Therefore, it was concluded that a linear fit of the R plot does not provide the required precision on y_{CP} measurements.
All the subsequent studies focused on the detector efficiency for D^0 decays and on its incidence on y_{CP} measurements. For what concerns the first, a small discrepancy was introduced between the efficiencies used for the reconstruction of $D^0 \to KK$ and $D^0 \to K\pi$. Then, by progressively varying the amplitude of such discrepancy, it was possible to quantitatively characterise how the variation of the detector efficiency (with respect to the two different decays) affects the measurement of y_{CP}. It was found that, to not violate the agreement of y_{CP} with its expected value, the highest order of magnitude for the efficiency difference is $O(10^{-5})$.
In the last part of the analysis, a correction for the efficiency was performed on the *reconstructed samples* of D^0 decays by applying weights to the events. In particular, through a proper choice of the efficiency profile for the correction, two separated studies assessed the effects of certain efficiency fluctuations on the measurement of y_{CP}. In the first, a statistical error was introduced on the efficiency profiles used in the correction. To accomplish this, the efficiency values applied to each bin were varied from one study to the other within a certain relative uncertainty (controlled by a small parameter θ). In this way, it was possible to calculate the bias on y_{CP} measurements caused by different statistical uncertainties on the efficiency (Table 2). In the second study, instead, the efficiency profile used for the correction of one of the two decays was varied through correlated fluctuations over the bins (while the efficiency for the second decay was maintained unchanged). In particular, two opposite fluctuations were applied: the first was higher on the first bin, then gradually decreased until it vanished on the last one; while the second was null on the first bin and maximum on the last one. By progressively varying the magnitude of the two fluctuations, it was observed that a variation of the efficiency at low D^0 decay-time is in general more significant than an analogous variation applied at the topmost region of the decay-time range.
In conclusion, the measurement of y_{CP} from a fit to the ratio R is feasible as long as we can control the efficiency fluctuations for the selected final states within a certain order of magnitude. Indeed, if a required precision on the measurement needs to be achieved, we have

to account for a certain systematic uncertainty due to the aforementioned fluctuations on the efficiency profiles. This analysis allows us to evaluate such uncertainty from the results in Table 2 and Table 3. In particular, the systematic error on y_{CP} related to the efficiency is given by the contribution of $\sigma_{y_{CP}}$ (Equation 15) in the first case, and σ_1 or σ_2 (Equation 17) in the second case. A further analysis would be needed to understand which type of correlated fluctuation has the highest impact on the detection efficiency - namely, which value between σ_1 and σ_2 has to be considered. However, thanks to the studies performed, it is already possible to estimate the order of magnitude of the error on y_{CP} caused by a certain relative uncertainty on the efficiencies.

6 References

[1] L. collaboration, R. Aaij, C. A. Beteta, *et al.*, "Observation of CP violation in charm decays", *Physical Review Letters*, vol. 122, no. 21, p. 211 803, May 2019, arXiv: 1903.08726, ISSN: 0031-9007, 1079-7114. DOI: 10.1103/PhysRevLett.122.211803. [Online]. Available: http://arxiv.org/abs/1903.08726 (visited on 06/04/2019).

[2] M. Kobayashi and T. Maskawa, "CP-Violation in the Renormalizable Theory of Weak Interaction", en, *Progress of Theoretical Physics*, vol. 49, no. 2, pp. 652–657, Feb. 1973, ISSN: 0033-068X. DOI: 10.1143/PTP.49.652. [Online]. Available: https://academic.oup.com/ptp/article/49/2/652/1858101 (visited on 06/07/2019).

[3] M. T. Alexander, "Constraints on Mixing and CP-Violation in the Neutral Charmed Meson System at LHCb", en, p. 228,

[4] L. collaboration, R. Aaij, C. A. Beteta, *et al.*, "Measurement of the charm-mixing parameter y_{CP}", en, *Physical Review Letters*, vol. 122, no. 1, p. 011 802, Jan. 2019, arXiv: 1810.06874, ISSN: 0031-9007, 1079-7114. DOI: 10.1103/PhysRevLett.122.011802. [Online]. Available: http://arxiv.org/abs/1810.06874 (visited on 05/27/2019).

[5] The LHCb collaboration, R. Aaij, C. A. Beteta, *et al.*, "Measurement of mixing and CP violation parameters in two-body charm decays", en, *Journal of High Energy Physics*, vol. 2012, no. 4, Apr. 2012, ISSN: 1029-8479. DOI: 10.1007/JHEP04(2012)129. [Online]. Available: http://link.springer.com/10.1007/JHEP04(2012)129 (visited on 05/27/2019).

[6] *Charm physics — Heavy Flavor Averaging Group*. [Online]. Available: https://hflav.web.cern.ch/content/charm-physics (visited on 06/04/2019).

[7] "The LHCb Detector at the LHC", p. 217, 2008.